This is a preprint, the final version is subject to change, of the American Mineralogist (MSA)
Cite as Authors (Year) Title. American Mineralogist, in press.
(DOI will not work until issue is live.) DOI: http://dx.doi.org/10.2138/am.2014.4589 12/11
Correction 28th November 2013

Infrared absorption spectroscopy of SiO_2-moganite

Ming Zhang[1, 2],* Terry Moxon[3]

[1] Frontier Institute of Science and Technology, Xi'an Jiaotong University,
710054, Xi'an, China
[2]Department of Earth Sciences, University of Cambridge,
Downing Street, Cambridge CB2 3EQ, UK
[3]55 Common Lane, Auckley, Doncaster DN9 3HX, UK

*Corresponding author, E-mail: mzhanguk@gmail.com

ABSTRACT

Moganite, a newly approved mineral, is microcrystalline silica. Samples of microcrystalline silica varieties containing variable amounts of moganite have been analysed using absorption infrared spectroscopy (IR). The main spectral differences between moganite and α-quartz occur in the wavenumber region below 650 cm^{-1}. Above this wavenumber, the frequencies of Si-O stretching vibrations of moganite are almost identical to those of quartz. Additional moganite bands were recorded near 165, 207, 296, 343, 419, 576 and 612 cm^{-1}, and several of these extra IR bands have been identified for the first time in moganite. The results indicate that moganite and quartz have different crystal structures and symmetries in terms of different tetrahedral linkages. Infrared spectra obtained from samples with different moganite contents cannot be simply explained by mechanical mixing of the two moganite and quartz end phases. The change in moganite content leads to not only a variation of spectral intensity, but also a systematic modification in band position and full width at half maximum. This unusual behaviour is attributed to grain size, strains and stacking faults in moganite and the intergrowth of moganite with fine-grained quartz. The close correlation between band width and moganite content is indicative of an improved crystallinity with decreasing in moganite concentration that has been identified in natural quartz variations. The results imply that moganite may play a role in the formation or crystallization of microcrystalline quartz. The present IR application offers a new method to estimate the moganite content in microcrystalline silica varieties.

INTRODUCTION

Moganite is a microcrystalline silica polymorph (Flörke et al. 1984). It has recently been approved as a valid mineral species (CNMMN no 99-035) by the Commission on New Minerals and Mineral Names of the International Mineralogical Association. The crystal structure of moganite has been described as monoclinic (Miehe et al. 1988) with alternate stacking of layers of $[10\,\bar{1}\,1]$ slices of left- and right-handed α-quartz corresponding to a periodic Brazil-law twinning on the unit-cell scale (Miehe and Graetsch 1992). Moganite is reported to have cell parameters of a = 8.758, b = 4.876, c = 10.715 Å, and β = 90.08° and space group $I2/a$ (Z = 12) (Miehe and Graetsch 1992), compared with a = 4.913, b = 4.913, c = 5.404 Å, and space group $P3_121$ (Z = 3) for α-quartz (Deer et al. 1992). Physical properties and crystal structure of moganite have been explored by some investigators (Graetsch et al. 1987; Miehe and Graetsch 1992; Graetsch et al. 1994; Petrovic et al. 1996; Götze et al. 1998; Heaney and Post 2001; Hantsch et al 2005; Heaney et al. 2007). Moganite is found to coexist and form intergrowths with fine-grained quartz varieties, e.g., chert, agate and chalcedony from around the world (Heaney and Post 1992; Parthasarathy et al. 2001; Rodgers and Cressey 2001; Moxon and Ríos 2004). Moganite-type phases have been identified in the silica analog phosphorus oxynitride (PON) (Chateau et al. 1999), zinc borophosphate (Huang et al. 2008) and $AlPO_4$ (Kanzaki and Xue 2012).

Quartz shows a varied distribution and high abundance in the Earth's rocks. Hence, a better understanding of the structural relationship with other minerals is of scientific interest. The relatively recent discovery of moganite means that knowledge of its optical properties [such as infrared (IR) spectra] and comparison with other well known crystalline polymorphs of silica may offer important information on the degree of diagenesis in microcrystalline silica. Moganite is suggested as an indicator for crystallization in evaporitic environments (Heaney 1995). Although IR spectra of moganite have been reported by several groups, the spectra acquired in these investigations offered limited lattice phonon modes and some were mainly focused on the

near infrared (NIR) region (Graetsch et al. 1987; Miehe and Graetsch 1992; Graetsch et al. 1994; Parthasarathy et al. 2001; Zhang and Moxon 2012; Hardgrove and Rogers 2013). Additionally, some of the previously reported infrared spectra of moganite showed inconsistent features. For example, the work of Parthasarathy et al. (2001) gave a relatively strong IR band near 600 cm^{-1}; however, this absorption was not clearly revealed in the study of Miehe and Graetsch (1992). There was also a lack of comprehension or detailed analysis on how IR spectra may change with varying moganite content. Therefore, the present study also aimed to gain a good understanding of the vibrational phonons of moganite, and to compare the spectral differences or similarities between moganite and quartz. A prime aspect of the investigation was the varying level of intergrowth between moganite and quartz and the possible effect on the spectral features.

Although signals of moganite have been detected in synthesised nanocrystalline SiO_2 (Schäf et al. 2006), the sample was far from a pure moganite phase and there has been no report on successful synthesis of pure SiO_2 moganite. In order to identify the characteristic vibrations of moganite, this investigation was extended into additional analyses of silica minerals in which moganite is commonly found: chert, flint, agate and chalcedony (Heaney and Post 1992). For the present study, we report the most complete infrared analysis of moganite to date and link its spectral similarities and differences with quartz. The results also provide a new spectroscopic method to estimate the moganite content in microcrystalline silica varieties.

BACKGROUND INFORMATION ON THE MINERALS

An extensive powder X-ray diffraction examination of more than 150 samples of microcrystalline quartz varieties (flint, chert, chalcedony and agate) demonstrated that most samples contained moganite (Heaney and Post 1992). It was proposed that high concentration of moganite in chert is an indicator for crystallization in evaporitic environments (Heaney 1995). However, the most moganite-enriched material (65–85%) was found in the ignimbrite lava flows of the Mogan Formation, Gran Canaria. Chemical analysis of Gran Canaria moganite (Petrovic et

al. 1996) has shown that Al and Na are the main impurities (at 0.33 and 0.30 wt%, respectively). Other common elements (such as Fe, K, Ca, Mg and Mn) only occur at trace levels.

Petrographic classification of the microcrystalline varieties of the quartz family (flint, chert, chalcedony and agate) is partly based upon the different textural types which may be associated with different growth conditions and chemical compositions. Flint and jasper are typically granular with chalcedony and agate showing mainly a fibrous structure. Banded chalcedony is known as agate and can be found in igneous and sedimentary environments. More detailed information regarding the classification of fine-grained silica can be found in previous studies (e.g., Frondel 1962; Flörke et al. 1982).

Moganite is believed to appear in the final stages during the diagenesis of amorphous silica. Diagenetic transformations have been discussed in relation to many siliceous deposits e.g. biogenic silica (Bohrmann et al. 1994), and siliceous sinters (Rodgers et al. 2004). Extensive experimental work has been undertaken to determine the effects of temperature and/or pressure on a variety of silica starting materials eventually producing α-quartz [e.g., Kieselgel, Mizutani (1966); silica gel, Oehler (1976); fumed silica, Bertone et al. (2003); diatomite, Huang (2003)]. The final outcome of these field and experimental studies has resulted in a consensus regarding the development of chert and silica sinter as follows: opal-A (amorphous silica) → opal-CT (poorly crystalline cristobalite and tridymite) → opal-C (cristobalite) → (± chalcedony) → granular α-quartz (von Rad and Riech 1979; Williams et al. 1984; Rodgers et al. 2004). There is, however, less agreement regarding the origin of agate, although a similar diagenetic pathway seems most likely (Landmesser 1998; Moxon and Carpenter 2009; Moxon et al. 2013). The role of moganite in the above diagenetic change remains unclear.

SAMPLES and EXPERIMENTAL METHODS

Moganite and microcrystalline quartz samples

A group of microcrystalline silica samples with different concentrations of moganite and microcrystalline quartz was analysed to reveal spectral changes caused by variations in moganite content. In this study, samples with high moganite (70-89%) are referred to as "moganite". The natural polycrystalline samples (Table 1) are from sedimentary and igneous hosts of different ages. They include agate from Australia, Brazil, Mexico, Scotland, USA; chert and flint from England; and moganite from Gran Canaria, Spain. Most of these samples have been previously characterized (Moxon and Ríos 2004; Moxon and Carpenter 2009; Zhang and Moxon 2012). Here, we have followed the division of siliceous sediments as described by Tucker (1991) into chert (found in limestone) and flint (found in European chalk from the Upper Cretaceous Period). A quartz standard (originally a single crystal) was also investigated by infrared spectroscopy, allowing a comparison between moganite and microcrystalline quartz. The standard or single crystal quartz is here described as macrocrystalline quartz. IR data from the present study indicates that well-crystallized and moganite-free microcrystalline quartz, such as Kil5, has IR spectra very similar to that of the quartz standard.

X-ray diffraction (XRD)

Measurement of accurate powder XRD intensities requires a grain size of < 10 μm (Bish and Reynolds 1989). A portion of each sample was first hand-ground and sieved to obtain grain sizes < 52 μm. A fixed mass of the sieved powder was then mixed with ethanol and ball-mill ground to produce powders in the 4 to 10 μm range. Diffraction patterns were obtained from these powders using a Bruker D8 diffractometer in reflection mode. Preliminary scans over the $16° < 2\theta < 52°$ range provided initial identification of the mineral phases that were present.

Most agates contain moganite but the determination of low levels using Rietveld refinement is imprecise due to an overlap of the moganite and quartz peaks. An alternative estimation of the moganite content has been discussed (Moxon and Ríos 2004; Moxon and Carpenter 2009), and is used for the present study. Diffraction patterns were collected over the range $17° < 2\theta < 25°$

using a step size of 0.02° and a scan rate of 20 s/step. This scan range includes the strongest moganite peaks at ~20° and the (100) quartz peak at 20.84°. The moganite and quartz peak areas were determined by fitting two unconstrained Lorentzian functions using the Advanced Fitting Tool in "OriginLab" and the total area was obtained using the baseline tool. The moganite content has been taken as the proportion (in %) of peak area moganite / total peak area, with an estimated uncertainty of ±2%.

Infrared analysis

IR powder and thin section absorption techniques were used in the present study. For powder absorption measurements, the pellet method reported by Zhang et al. (1996) was employed. The textural features of the samples are not expected to cause issues in the present results, because the data were mostly from finely powdered samples with randomly orientated micro grains. Fine sample powders were thoroughly mixed with dry KBr powders (at a sample-to-KBr ratio of 1:300, 1:500 and 1:750) or polyethylene powders (sample-to-polyethylene ratio = 1:50). 200 mg (for KBr) or 100 mg (for polyethylene) of the mixtures were pressed into 13 mm diameter disks under vacuum. Doubly polished thin sections of polycrystalline samples (with thicknesses of 69, 98, 130, 320 μm and 1.5 mm) were used to record weak absorption bands in low wavenumber and NIR regions.

IR data acquisition was carried out using Bruker IFS 113v and Bruker IFS 66v spectrometers with similar methods as reported in Zhang and Salje (2001). A Globar lamp, a KBr beam splitter, and a DTGS detector were used to record data in the MIR region, whereas a mercury or Globar lamp, 3.5-μm and 23-μm Mylar beam splitters and a DTGS detector were used to collect data down to 20 cm^{-1} in the FIR region. All data were acquired in vacuum with an instrumental resolution of 2 cm^{-1} as better resolution did not improve the spectral details. The OPUS-IR (Bruker) software was used for data analysis. Band or peak parameters, such as band position, intensity (height), area and width (or full width at half maximum, FWHM), were determined by

curve fitting with Lorentzian function. The analysis error is less than 5% for band intensity and area, less than 1 cm^{-1} for FWHM and band position. Additionally, the 2nd-derivitive method was also used for peak analysis.

RESULTS

XRD analysis

Typical XRD results are shown in (Fig. 1). The only mineral phases identified by XRD in our samples were moganite and quartz (Table 1). An independent analysis using Rietveld refinement was carried out on the Hunstanton flint sample (Huns 16) by F. Matteucci (personal communication). The moganite content was estimated at 15(5)% and this compares with the value of 18(2)% determined in the present study.

The collected data allow a moganite content division into four groups: a) > 50 wt% moganite content with samples only from Mogan, Gran Canaria; b) 20 to 10 wt% shown by flint from Dorset and Norfolk, England together with agate from Nebraska, USA and Rio Grande do Sul, Brazil; c) 10 to 5 wt% found in flint from Yorkshire, England and agate from Laguna, Mexico and Agate Creek, Australia; d) < 5 wt% found in chert from Derbyshire, England and agate from Ardownie, Scotland and Killara, Western Australia (Table 1).

XRD data analysis (Fig. 1) showed that the moganite peaks at ~20° 2θ exhibited a systematic change in peak width, i.e., samples (e.g., BDL10) with high moganite content have diffraction patterns clearly broader and noisier than those with low moganite concentration or the moganite free samples (e.g., Kil5).

Infrared absorption spectra of moganite

Moganite is considered to have a monoclinic crystal structure. Based on the symmetry (*I*2/*a* or *C*2/*c*) of moganite proposed by Mieche et al. (1988), the irreducible representation for optical modes of moganite was suggested as $13A_g$ (R) + $12A_u$ (IR) + $14B_g$ (R) + $12B_u$ (IR) (Kingma and

Hemley 1994), where R indicates Raman-active optical modes and IR represents infrared-active modes. 24 IR-active modes ($12A_u + 12B_u$) and 27 Raman-active modes ($13A_g + 14B_g$) are to be expected in moganite. In contrast, quartz has a trigonal symmetry ($P3_121$), and nine atoms per primitive cell. Factor group analysis shows that quartz has sixteen optical vibrations, $4A_1$ (R) + $4A_2$ (IR) + $8E$ (IR and R) (e.g., Scott and Porto 1967). Therefore, there are only 12 IR and 12 Raman modes in quartz. Infrared vibrational modes of quartz have been well investigated using reflection and absorption techniques (e.g., Spitzer and Kleinman 1961; Gervais and Piriou 1975; Salje et al. 1992).

Figures 2 and 3 show IR absorption spectra of samples with various moganite contents. These plotted spectra are mainly arranged according to their spectral broadness and the concentration of moganite determined by XRD (Table 1). The IR data (Figs. 2a–3b) show clearly that moganite (e.g, BDL10) and quartz or well-crystallized microcrystalline quartz (e.g., Kil5, which is essentially moganite-free) have different vibrational spectra, indicative of different crystal structures. Detailed band assignments for moganite have yet to be established. Nevertheless, the observed bands in the present study can be classified into several groups based on the general understanding of vibrational spectra of silica or silica-like materials (e.g., Soda 1961, Etchepare et al. 1974 and 1978; Sato and McMillan 1987; Kingma and Hemley 1994; Cellai et al. 1995; Zhang et al. 2003; Zhang and Scott 2007; Coh and Vanderbilt 2008). The bands above 600 cm^{-1} are expected to be Si-O stretching vibrations, and those in 300–600 cm^{-1} are mainly associated with bending of SiO_4 tetrahedra. The bands below 300 cm^{-1} may mainly involve bending, translations and rotations of SiO_4 tetrahedra.

As explained earlier, one of the main objectives of the present study was to determine and investigate characteristic vibration modes of moganite. However, the band identification was not straightforward, because of the coexistence of quartz even in moganite-rich samples, and also because almost identical spectral features exist between moganite-rich samples and standard quartz above 650 cm^{-1} (Fig. 3a). In order to ensure good clarification, different techniques were

used and a large number of samples with varying moganite content were measured and analysed (Figs. 4–6).

The identification of characteristic modes in moganite was mainly based on two types of individual band behaviour: (1) the appearance of additional bands which do not exist in quartz and whose intensities show a clear increase with increasing moganite concentration (e.g., Fig. 2b, c, 4c); and (2) bands with frequencies similar to those in quartz, but without a tendency to disappear in moganite-rich samples (e.g., Fig. 4a, d, e). As a result, a total of 16 IR bands were clearly identified as characteristic vibrations of moganite and this excluded 3 very weak bands with frequencies similar to those of quartz. The frequencies of observed IR bands in moganite (such as BDL10 and BDL11) are listed in Table 2 together with previous observations. The data in Table 2 are also compared with IR bands observed in microcrystalline quartz (sample Kil5) and standard quartz, as well as previously published IR data of cristobalite (Zhang and Scott 2007) and tridymite (Plendl et al. 1967).

Moganite showed several additional IR bands that are commonly absent in quartz or well-crystalline microcrystalline quartz The bands are found at 296, 343, 576 and 612 cm^{-1} with the 612 cm^{-1} band being particularly weak (Table 2, Figs. 2a, 2b, 3a, 3b, and 4c). Data from thin section samples (98μm thick Mog7 and 320 μm thick BDL 1) showed two extra weak bands at 165 and 207 cm^{-1} (Table 2, Fig. 2c). These two low-wavenumber bands are likely to involve different translational and rotational vibrations of SiO_4 tetrahedra as compared with other silica phases (e.g., Soda 1961; Etchepare et al. 1974 and 1978; Sato and McMillan 1987). It is interesting to note that quartz also has a band near 207 cm^{-1} but it is A_1 symmetry (only Raman active) and not infrared active (Scott and Proto 1967). These observed additional IR bands, which are absent in quartz, are all located below 650 cm^{-1} (Fig. 3b). They involve formations or modifications associated with bending, translational and rotational vibrations of SiO_4 tetrahedra: indicative of additional tetrahedral linkage(s) as previously revealed by NMR (Graetsch et al. 1994).

The IR measurements did not show detectable IR bands between 20 and 120 cm^{-1} in moganite. In a slightly higher wavenumber region, a broad feature (near 124 cm^{-1} in BDL10, and near 127 cm^{-1} in BDL1) was detected in moganite. Although quartz has a very weak infrared mode (*E* symmetry) at 128 cm^{-1} (Table 2), the Raman data reported by Kingma and Hemley (1994) showed a strong Raman band at 129 cm^{-1} in a moganite-rich sample. On this evidence, moganite could have an IR band near 128 cm^{-1}. Another weak band was detected in all samples near 264 cm^{-1} (Figs. 2a–2c). This band was found near 257 cm^{-1} in high moganite samples such as BDL10. This is interesting as macrocrystalline quartz also has a band with this wavenumber (Table 2). The intensity of this band remained relatively intense in moganite-rich samples, and this suggests the band should be a characteristic band of moganite. This conclusion is further supported by results from reflectance spectra (the reflectance data will be published as a separate work).

The data show that most IR modes of quartz appear active in moganite and were particularly intense in the moganite-rich samples, thus reflecting the close connection between the crystal structures of the two minerals (Table 2, Figs. 2a, 2b, 3a and 3b). However, there are two IR modes at 371 and 397 cm^{-1} showing a dramatic drop in intensity (85–90%) with increasing moganite content (Fig. 2a). The 371 cm^{-1} band is located near 375 cm^{-1} in microcrystalline quartz samples and it shifts gradually to the lower wavenumber in moganite (Fig. 2a). This behaviour seems to suggest their disappearance when extrapolating to pure moganite (Fig. 4b). As quartz has characteristic bands at 371 (A_2) and 397 cm^{-1} (*E* mode) (Table 2), the significant change implies that they may be due to the coexistence of microcrystalline quartz in the samples, and these two bands may not be characteristic bands of moganite. However, the Raman work of Kingma and Hemley (1994) identified a vibration at a similar wavenumber (398 cm^{-1}) for moganite. Therefore, the nature of the 397 cm^{-1} IR band in moganite-rich samples remains unclear and it is not listed as a characteristic IR band of moganite in Table 2.

The IR spectra of the samples exhibit a gradual sharpening of the bands with decreasing moganite content. This is especially pronounced for bands near 264 and 696 cm^{-1} (Figs. 2b, 3a, 5a and 5d) and the Si-O stretching band near 1169 cm^{-1} (Fig. 3a). The 1169 cm^{-1} band showed the strongest broadening variation (Fig. 3a). In contrast to these bands, the absorption feature near 576–585 cm^{-1}, which is absent in moganite-free microcrystalline quartz (Kil5) and yet it is relatively intense in moganite-rich samples (Figs. 3a and 3b), showed a significant change in intensity, wavenumber and width with decreasing moganite concentration (Figs. 4c, 5c and 6). The wavenumber shifted from 576–585 cm^{-1} down to 554–556 cm^{-1} in moganite-poor samples (samples Br36 and AgCr85 in Fig. 3b). Its band intensity exhibited a linear correlation with the moganite content determined by XRD in the low moganite content region (Fig. 4c). However, the data points become more scattered in samples with high moganite concentrations. This observed correlation between moganite content and IR band profile (Figs. 4–5) can be used for an estimation of moganite concentration in microcrystalline silica varieties. The advantage of the IR application is that it uses a small amount of sample (e.g., 2 mg in 100 mg polyethylene for FIR measurements or 0.4 mg in 200 mg KBr for MIR measurements) and the correlation length of the technique is on the scale of the unit cells. This means that IR spectroscopy is sensitive to short- and intermediate-range order. The latter is different for moganite and quartz (Kingma and Hemley, 1994). For example moganite contains four-membered rings of SiO_4 tetrahedra, which absent in the structure of quartz. Therefore IR spectroscopy has the potential to detect and determine the amount of moganite on the basis of vibrational modes generated by the structural species representative for the intermediate range order. In this sense, IR spectroscopy compares favourably to XRD because in general XRD requires repetition of more than 10 unite cells to generate detectable Bragg reflection. In the case of moganite-quartz samples, the discrimination of the two phases by XRD is further hindered by the similarity of their long-range order. A recent IR work on chalcedony by Schmidt and Fröhlich (2011) recorded a weak absorption feature near 555 cm^{-1}, and attributed it to free Si-O vibrations in non-bridging Si-OH groups (surface silanol).

One other assignment for this band is that it is a possible vibration of moganite, because the present study has demonstrated that this 576 cm^{-1} moganite band falls to 555–556 cm^{-1} in moganite-poor samples (Figs. 3b) and also chalcedony contains moganite. Similar absorption in the wavenumber region has been reported in ZSM-type zeolite and is indicative of the existence of corresponding building units (Coudurier et al. 1982), rather than Si-OH groups.

Interestingly, a weak absorption occurred near 610–612 cm^{-1} is found in all samples, except sample Kil5 (which is moganite-free) and the standard quartz sample. It was tempting for us to consider this band as a multi-phonon absorption, because of its weak intensity. However, moganite samples from the Deccan flood basalts of the Killari area, Maharashtra, India (Parthasarathy et al 2001) show a relatively intense band near this wavenumber, eliminating the signal as a multi-phonon band. This feature is listed as a characteristic band of moganite in Table 2, but its vibrational nature has not been established. Crystalline silica can have infrared bands in this wavenumber region as shown by the weak absorption bands of cristobalite and tridymite with the respective peaks at a slightly higher wavenumber of ~617 and 620 cm^{-1} (Table 2).

The IR absorption data of moganite in the present study are similar to those reported by Miehe and Graetsch (1992), who also measured moganite samples from Gran Canaria and whose data were in a limited wavenumber region and also did not reveal some weak bands (e.g., 612 cm^{-1}). The IR spectrum of moganite detected in chalcedony found in the Indian Deccan flood basalts from Killari, Maharashtra shows a strong and broad absorption near 600 cm^{-1}, whereas the band near 570 cm^{-1} is very weak but relatively sharp (Parthasarathy et al. 2001). Contrarily, this intense 600 cm^{-1} absorption was not observed in any of our samples. The moganite bands with the closest frequencies in our data are near 610 and 612 cm^{-1}. Further differences between the Killari and Gran Canaria moganites are (i) Killari moganite has bands at 800 and 808 cm^{-1}, which are in contrast to the similar bands near 780 and 798 cm^{-1} in quartz and moganite samples from Gran Canaria (Table 2); (ii) The Killari samples did not show a band near 343 cm^{-1} which

318 was clearly recorded in the Gran Canaria moganite (Mog 12, BDL 10, Fig. 2b) and further
319 identified in microcrystalline quartz, e.g. Neb 1 and Wh No 3 (Fig 2b).

320 Absorption spectra of multi-phonon modes of moganite (BDL10) were recorded and are
321 shown in Figure 7a. The data reveal relatively strong bands at 1491, 1526, 1611, 1682, 1787,
322 1864, and 1955 cm^{-1}. Its 2nd-derivative spectrum is given to show more detailed positions of the
323 multi-phonon modes (Fig. 7b). The wavenumber of the 1491 cm^{-1} implies that it is most likely
324 due to a combination process of the 696 and 798 cm^{-1} bands (696 + 798 = 1494), whereas the
325 1526 cm^{-1} multi-phonon absorption is related to the 448 and 1082 cm^{-1} bands (448+ 1082 =
326 1530). More detailed assignments mainly based on absorption frequencies are given in Table 3.

327 Moganite (BDL10) shows O-H stretching vibrations near 3440 and 3586 cm^{-1} (Fig. 8). The
328 former is due to absorbed H_2O. The latter band is relatively sharp, indicating that it most probably
329 arises from OH or silanol (Si-OH) which are structural defects. The combination bands (O-H
330 stretching + Si-O-H bending) associated with the OH species occur as a broad feature with
331 absorption local maxima at 4356, 4405, 4442, and 4498 cm^{-1} shown by the 2nd-derivative
332 method. The data suggest that the bending vibrations should be located in 800–920 cm^{-1}. The
333 powder absorption spectra (sample BDL10 with KBr ratio = 1 : 300) of moganite showed a weak
334 broad feature extending over 850–930 cm^{-1} with a local absorption maximum near 892 cm^{-1}. This
335 feature is considered as the Si-O-H bending. The combination mode that includes stretching and
336 bending of H_2O is recorded near 5226 cm^{-1} while the bending mode of H_2O was identified near
337 1600 cm^{-1} using the KBr pellet samples. The first overtones of the H_2O and OH stretching are
338 located near 6828 and 7040 cm^{-1}, respectively.

339

340 **DISCUSSION**

341 One important issue associated with our observation is the origin of spectral broadening in
342 moganite-rich samples and its implications. Moganite-rich samples with a moganite content of
343 74–89 wt% exhibit IR band FWHM about three to four times larger than those in moganite-poor

or moganite-free samples (Figs. 5a–e). The broadening is associated not only with those bands that are characteristic for both moganite and quartz (e.g., bands at 264, 696, and 797 cm^{-1}), but also of moganite-only bands (576 cm^{-1}) and quartz-only bands (374 cm^{-1}). Similar broadening has been reported by other studies using different analytical methods. For example, Graetsch et al. (1994) found that the ^{29}Si MAS NMR signals of moganite and chalcedony were at least five times broader than the resonance signals of pure quartz powder. The sample powdering processes used in the present study could potentially cause defects and structural damage and consequently affect the powder IR absorption spectra. However, this was not a problem as demonstrated by IR reflection spectra recorded from large bulk moganite samples showing a similar degree of broadening. Hence, the band broadening had not been introduced by the powdering processes. A recent study investigated the crystallite size, microstrain, stacking disorder and moganite content in flint and other chert raw materials using X-ray powder diffraction profile analysis (Graetsch and Grünberg 2012). These authors interpreted the observed broadening in X-ray reflections of the quartz varieties to be due to both anisotropic small crystallite size and anisotropic microstrain. The systematic broadening revealed by various analytic methods with different correlation length scales seems to indicate that high moganite samples are likely to have a defect structure associated with very poor crystallinity. It has been reported that moganite-rich samples tend to have nano scale grain sizes or textures (Miehe and Graetsch 1992; McKnight et al. 2008). This may partly be responsible for the changes in band profiles with concentration. The effect of grain size and strain on vibrational spectra has been previously demonstrated and a deviation from a linear relationship of absorbance to concentration was produced (Tuddenham and Lyon 1960; Coudurier et al. 1982; Tamura and Ichinokawa 1983). Relatively high hydrogen contents might also have influence on the band parameters. Graetsch et al. (1994) and Zhang and Moxon (2012) have reported about 2-4 wt% H_2O in the formation of OH and H_2O in moganite. Further investigations to look into these issues are desirable. The present study also shows that the IR spectra of the samples exhibit not only variations in band intensity and width with decreasing

370 moganite content, but also an unusual modification in band wavenumber, especially between 450
371 and 600 cm^{-1} (Fig. 3b). For example, the IR band near 576 cm^{-1} shows a change of about 20-30
372 cm^{-1} in wavenumber with the changing moganite content (Fig. 3b). These significant
373 wavenumber variations cannot be created by simply mixing or combining the spectra of moganite
374 and quartz in different proportions. Changes in band frequencies generally indicate variations
375 with energies of corresponding vibrations or bonding. The length scale is only a few unit cells of
376 infrared spectroscopy, and the reported intergrowth of moganite with microcrystalline quartz is at
377 the unit-cell level (Heaney and Post 1992). Hence, an apparent implication of the IR results is that
378 the intergrowth of moganite with quartz might also affect the local structure involving the
379 damping and energies of vibrational modes. Consequently, moganite intergrowths can modify all
380 the modes in the IR spectra. The correlation shown in Figs. 4 and 5 might imply that natural
381 moganite also has a diagenetic relation with quartz, i.e., moganite plays an important role in the
382 transformation of amorphous silica to microcrystalline quartz.
383 In summary, the present study shows that there are both spectral similarities and differences
384 between moganite and macrocrystalline or microcrystalline quartz. Although the two materials
385 have different crystal structures, moganite and quartz have almost identical band frequencies in
386 the region of 650–1200 cm^{-1}. Their main spectral differences occur in the FIR region where the
387 Si-O-Si bending, translation and rotations of SiO_4 are commonly located. Characteristic bands of
388 both materials become relatively sharp when there is less moganite in the sample. The spectral
389 changes in the samples do not follow the behaviour of a mechanical mixing of the two phases.
390 This is clearly demonstrated by the phonon frequencies and widths of characteristic bands of
391 moganite (e.g., the 675 cm^{-1} band) showing a shift with change of moganite concentration. The
392 results offer clear evidence that the crystal structure of moganite is a modification from that of
393 quartz at a level of a few unit cells; this might involve different linkage of SiO_4 tetrahedra, stack
394 faults, twins and bonding angles.

The results from the present study have important implications allowing moganite to be used for the identification of evaporites and to measure the degree of diagenesis in microcrystalline silica. The IR data, especially in the FIR region where several moganite bands were revealed for the first time, may be very useful in identifying moganite and determining its content in quartz varieties. In these spectroscopic applications, one of the key and essential issues is the behaviour of vibrational modes of moganite as a function of content. The observed non-linear changes in some modes of moganite and microcrystalline quartz as a function of concentration imply that the recorded IR, and possibly Raman, spectroscopic intensity of moganite may be associated with not only its concentration, but also other factors such as grain size. Therefore, when the band intensity of moganite or intensity ratio between moganite and quartz is used to extract concentrations, the non-linear behaviour observed in the mixing may need to be considered. The systematic spectral changes of microcrystalline quartz with moganite concentration demonstrate that the two minerals have not only a close relation in crystal structures, but also a genesis link. Moganite is an important stage or an intermediate phase in the formation of microcrystalline quartz. The transformation might take place structurally through removing or healing the periodic Brazil-law twinning and stacking faults in moganite during physical processes or over geological time resulting in a growth of the quartz crystallinity at the expense of moganite.

ACKNOWLEDGEMENTS

The authors are grateful to Peter Heaney and Jeffrey Post for providing us with the moganite samples, and to Roger Clark, Brad Cross, Nick Crawford, Brian Leith, and Dave Nelson for the agate and chalcedony samples used in the present study. We are much obliged to Tony Abraham, Department of Earth Sciences, Cambridge University for help in the XRD data collection. Francesco Matteucci kindly carried out an independent Rietveld refinement on a flint sample. We thank Peter Heaney, Thorsten Geisler, and Associate Editor Boriana Mihailova, for their constructive and helpful reviews and comments on the manuscript. The work is supported by the National Science Foundation of China (41372055)

REFERENCES CITED

Bertone, J.F., Cizeron, J., Wahi, R.K., Bosworth, J.K. and Colvin, V.L. (2003): Hydrothermal synthesis of quartz nanocrystals. Nano Letters, 3, 655–659.

Bish, D.L. and Reynolds, R.C. Jr. (1989) Sample preparation for X-ray diffraction. Reviews in Mineralogy, 20, 73–99.

Bohrmann, G., Abelmann, A., Gersonde, R., Hubberten, H. and Kuhn, G. (1994) Pure siliceous ooze, a diagenetic environment for early chert formation. Geology, 22, 207–210.

Cellai, D, Carpenter, M.A., Kirkpatrick, R.J., Salje, E.K.H. and Zhang, M. (1995) Thermally Induced Phase transitions in Tridymite: An Infrared Spectroscopy Study. Physics and Chemistry of Minerals, 22, 50–60.

Chateau, C., Haines, J., Léger, J-M, LeSauze, A., Marchard, R. (1999) A moganite-type phase in the silica anlog phosphorus oxynitride. American Mineralogist, 84, 207–210.

Coh, S. and Vanderbilt, D. (2008) Structural stability and lattice dynamics of SiO_2 cristobalite. Physical Review B, 78, 054117.

Coudurier, G., Naccache, C., Vedrine, J.C. (1982) Uses of I.R. spectroscopy in identifying ZMS zeolite structure. Journal of the Chemical Society, Chemical Communications, Issue 24, 1413–1415.

Deer, W.A., Howie, R.A. and Zussman, J. (1992) *An Introduction to the Rock Forming Minerals*. Longman Sciences & Technical, 2nd ed., pp696

Etchepare, J., Merian, M., and Smetankine, L. (1974) Vibrational normal modes of SiO_2. I. α and β quartz. Journal of Chemical Physics, 60, 1873–1876.

Etchepare, J., Merian, M. and Kaplan, P. (1978) Vibrational normal modes of SiO_2. II. Cristobalite and tridymite. Journal of Chemical Physics, 68, 1531–1537.

Flörke, O.W., Köhler-Herbertz, B., Langer, K. and Tönges, I. (1982) Water in microcrystalline quartz of Volcanic Origin: Agates. Contributions to Mineralogy and Petrology, 80, 324–333.

Flörke, O.W., Flörke, G. and Giese, U. (1984) Moganite - A new microcrystalline silica-mineral. Neues Jahrbuch für Mineralogie. Abhandlungen, 149, 325–336.

Frondel, C. (1962) *The system of mineralogy*, *vol 3, Silica Minerals*. John Wiley and Sons Incorporated, New York.

Gervais, F. and Piriou, B. (1975) Temperature dependence of transverse and longitudinal optic modes in the α and β phases of quartz. Physical Review B, 11, 3944–3950.

Götze, J., Nasdala, L., Kleeberg, R. and Wenzel, M. (1998) Occurrence and distribution of 'moganite' in agate/chalcedony: a combined micro-Raman, Rietveld, and cathodoluminescence study. Contributions to Mineralogy and Petrology, 133, 96–105.

Graetsch, H.A. and Grünberg, J.M. (2012) Microstructure of flint and other chert raw materials. Archaeometry, 54, 18–36.

Graetsch, H., Flörke, O.W. and Miehe, G. (1987) Structural defects in microcrystalline silica. Physics and Chemistry of Minerals, 14, 249–257.

Graetsch, H., Topalovic, I. and Gies, H. (1994) NMR spectra of moganite and chalcedony. European Journal of Mineralogy, 6, 459–464.

Hantsch, U., Winkler, B., Pickard, C.J., Gale, J.D., Warren, M.C., Milman, V. and Mauri, F. (2005) Theoretical investigation of moganite. European Journal of Mineralogy, 17, 21–30.

Hardgrove, C. and Rogers, A. D (2013) Thermal infrared and Raman microspectroscopy of moganite-bearing rocks. American Mineralogist, 98, 78–84.

Heaney, P.J. (1995) Moganite as an indicator for vanished evaporates: a testament reborn? Journal of Sedimentary Research A, 65, 633–638.

Heaney, P.J. and Post, J.E. (1992) The widespread distribution of a novel silica polymorph in microcrystalline quartz varieties. Science, 255, 441–443.

Heaney, P.J. and Post, J.E. (2001) Evidence for an *I2/a* to *Imab* phase transition in the silica polymorph moganite at ~570 K. American Mineralogist, 97, 631–639.

Heaney, P.J., McKeown, D.A. and Post, J.E. (2007) Anomalous behaviour at the *I2/a* to *Imab* phase transition in SiO_2-moganite: An analysis using hard-mode Raman spectroscopy. American Mineralogist, 86, 1358–1366.

House, M. (1989) *Geology of the Dorset Coast.* The Geologists' Association, London. 170p.

Huang, W.L. (2003) The nucleation and growth of polycrystalline quartz: pressure effect from 0.05 to 3 GPa. European Journal of Mineralogy, 15, 843–853.

Huang, Y.X., Prost, Y., and Kniep, R. (2008) $Zn[BPO_4(OH)_2]$: A novel zinc borophosphate with the moganite topology. Chemistry-A European Journal, 14, 1757–1761.

Kanzaki, M. and Xue, X. (2012) Structural characterization of moganite-type $AlPO_4$ by NMR and powder X-ray diffraction. Inorganic Chemistry, 51, 6164–6172.

Kent, P. (1980) British Regional Geology, Eastern England from the Tees to the Wash, Institute of Geological Sciences, London. 155p.

Kingma K.J. and Hemley, R.J. (1994) Raman spectroscopic study of microcrystalline silica. American Mineralogist, 79, 269–273.

Kobberger, G. and Schminke, H.-U. (1999) Deposition of rheomorphic ignimbrite D (Mogán Formation), Gran Canaria, Canary Islands, Spain. Bulletin of Volcanology, 60, 465–485.

Landmesser, M. (1998) "Mobility by Metastability" in Sedimentary and Agate Petrology: Applications. Chemie der Erde, 58, 1–22.

McKnight, R.E.A., Moxon, T., Buckley, A., Taylor, P.A., Darling, T.W. Carpenter, M.A. (2008) Grain size depednece of elastic anomalies accompanying the a-b phase transition in polycrystalline quartz. Journal of Physics: Condensed Matter, 20, 075229.

Miehe, G., Grätsch, H., Flörke, O.W., Fuess, H. (1988) Die monokline Kristallstruktur des SiO_2-Minerals Moganit. (Abstr) Zeitschrift für Kristallographie, 182**,** 183–184.

Miehe, G. and Graetsch, H. (1992) Crystal structure of moganite: a structure type for silica. Europeans Journal of Mineralogy, 4, 693–706.

Mizutani, S. (1966) Transformation of silica under hydrothermal conditions. Nagoya University Journal of Earth Science, 14, 56–88.

Moxon, T. and Ríos, S. (2004) Moganite and water content as a function of age in agate: an XRD and thermogravimetric study. European Journal of Mineralogy, 16, 269–278.

Moxon, T. and Carpenter, M.A. (2009) Crystallite growth kinetics in nanocrystalline quartz (agate and chalcedony). Mineralogical Magazine, 73, 551–568.

Moxon, T., Petrone, M.C. and Reed, S.J.B. (2013) Characterization and genesis of horizontal banding in Brazilian agate: an X-ray diffraction, thermogravimetric and electron microprobe study. Mineralogical Magazine, 77, 227–248.

Oehler, J.H. (1976) Hydrothermal crystallization of silica gel. Geological Society of America Bulletin, 87, 1143–1152.

Parthasarathy, G., Kunwar, A.C., and Srinivasan, R. (2001) Occurrence of moganite-rich chalcedony in Deccan flood basalts, Killari, Maharashtra, India. European Journal of Mineralogy, 13, 127–134.

Petrovic, L., Heaney, P.J. and Navrotsky, A. (1996) Thermochemistry of the new silica polymorph moganite. Physics and Chemistry of Minerals, 23, 119–126.

Pinto, V.M., Hartman, L.A., Santos, J.O.S., McNaughton, N.J. and Wildner, W. (2011) Zircon U-Pb geochronology from the Paraná bimodal volcanic province support a brief eruptive cycle at ~ 135 Ma. Chemical Geology, 281, 93–102.

Plendl, J. N., Mansur, L. C., Hadni, A., Brehat, F., Henry, P., Morlot, G., Naudin, F., Strimer, P. (1967) Low temperature far infrared spectra of SiO_2. Polymorphs. J. Phys. Chem. Solids, 28, 1589–1597.

Rawson, P.F. (1992) The Cretaceous. p 355-388 in: *Geology of England and Wales.* Duff, P. McL., & Smith, A.J.(eds): The Geological Society, London.

Rodgers, K.A. and Cressey, G. (2001) The occurrence, detection and significance of moganite (SiO_2) sinters. Mineralogical Magazine, 65, 2, 157–167.

Rodgers, K.A., Browne, P.R.L., Buddle, T.F., Cook, K.l., Greatrez, R.A., Hampton, W.A., Herdianita, N.R., Holland, G.R., Lynne, B.Y., Martin, R., Newton, Z., Pastars, D., Sannazarro, K.L. and Teece, C.I.A. (2004) Silica phases in sinters and residues from geothermal fields of New Zealand. Earth Science Reviews, 66, 1–61.

Salje, E.K.H., Ridgwell, A., Güttler, B., Wruck, B., Dove, M.T. and Dolino, G. (1992) On the displacive character of the phase transition in quartz: a hard-mode spectroscopy study. Journal of Physics: Condensed Matters, 4, 571–577.

Sato, R.K. and McMillan, P. F. (1987) An infrared study of the isotope species of α-quartz. Journal of Physical Chemistry, 91, 3494–3498.

Schäf, O., Ghobarkar, H., Garnier, A., Vagner, C., Lindner, J.K.N., Hanss, J. and Reller, A. (2006) Synthesis of nanocrystalline low temperature silica polymorphs. Solid State Sciences, 8, 625–633.

Schmidt, P. and Fröhlich, F. (2011) Temperature dependent crystallographic transformations in chalcedony, SiO_2, assessed in mid infrared spectroscopy. Spectrochimica Acta Part A: Molecular and Biomolecular Spectroscopy, 78, 1476-1481.

Scott, J.F. and Porto, S.P.S. (1967) Longitudinal and transverse optical lattice vibrations in quartz. Phys Review, 161, 903–910.

Soda, R. (1961) Infrared absorption spectra of quartz and some other silica modification. Bulletin of the Chemical Society Japan, 34, 1491–1495.

Spitzer, W.G. and Kleinman, D.A. (1961) Infrared lattice bands of quartz. Physical Review, 121, 1324–1335.

Stevenson, I.P. and Gaunt, G.C. (1971) *Geology of the country around Chapel-en-le-Frith.* Memoir of the Geological Survey of Great Britain. HMSO, London. 444p.

Tamura, A. and Ichinokawa, T. (1983) Frequency spectrum of a small particle. Journal of Physics C: Solid State Physics, 16, 4779–4788.

Tucker, M.E. (1991) *Sedimentary Petrology*, Blackwell Scientific Publications, Oxford, UK, 260 p.

Tuddenhamm W.M. and Lyon, R.J.P. (1960) Infrared techniques in the identification and measurement of minerals. Analytical Chemistry, 32, 1630–1634.

von Rad, U., and Riech, V. (1979) Silica diagenesis in continental margin sediments off Northwest Africa, in *Initial reports of the Deep Sea Drilling Project*, vol. XLI, 879–905.

Williams, L.A., Parks, G.A. and Crerar, D.A. (1984) Silica diagenesis, I. Solubility controls. Journal of Sedimentary Petrology, 55, 301–311.

Zhang, M. and Moxon, T. (2012) In situ infrared spectroscopic studies of OH, H_2O and CO_2 in moganite at high temperatures. European Journal of Mineralogy, 24, 123–131.

Zhang, M. and Salje E. K.H. (2001) Infrared spectroscopic analysis of zircon: radiation damage and the metamict state. Journal of Physics: Condensed Matter, 13, 3057–3071.

Zhang, M. and Scott, J. F. (2007) Raman studies of oxide minerals: a retrospective on cristobalite phases. Journal of Physics: Condensed Matter, 19, no.275201.

Zhang, M., Wruck, B., Graeme–Barber, A., Salje, E.K.H., and Carpenter, M.A. (1996) Phonon-spectroscopy on alkali-feldspars: Phase transitions and solid solution. American Mineralogist, 81, 92–104.

Zhang, M., Xu, H., Salje, E.K.H., and Heaney, P.J. (2003) Vibrational spectroscopy of beta-eucryptite ($LiAlSiO_4$): optical phonons and phase transition(s). Physics and Chemistry of Minerals, 30, 457–462.

568 ***Figure captions***

569

570 Figure 1. Powder X-ray diffraction patterns with an increasing moganite content (a) → (d). (a)
571 Kil 5 reveals only α-quartz signals; (b) Br 36 showing moganite and α-quartz signals; (c) Neb 1
572 showing moganite and α-quartz; and (d) BDL10 white powder from moganite, Gran Canaria
573 demonstrating the high moganite content. Square root counts are used in order to minimise the
574 effect of the major quartz signal at 26.64^{o} 2θ.
575

576 Figure 2a. Powder FIR absorption spectra of samples with different moganite content in the
577 region of 80–415 cm^{-1} (symbol "+" indicate the characteristic bands of moganite near 296 and
578 343 cm^{-1}). The spectra are vertically shifted for clarity.

579

580 Figure 2b. Detailed change indicative of intensity changes of the characteristic band of quartz
581 near 373 cm^{-1} and the characteristic band of moganite near 296 and 343 cm^{-1}.

582

583 Figure 2c. IR bands near 165 and 207 cm^{-1} were revealed in high moganite thin section slabs
584 (BDL1 and Mog7). A very weak absorption is recorded near 124 or 127 cm^{-1}, but it is unclear
585 whether this band is due to moganite or quartz.

586

587 Figure 3a. Powder IR spectra in the MIR region (between 350 and 1500 cm^{-1}). The spectra are
588 vertically shifted for clarity.

589

590 Figure 3b. Spectra from 535 and 640 cm^{-1} to show the detailed change of the additional features
591 near 576 and 612 cm^{-1}.

592

593 Figure 4. Band intensity (height) and band area as a function of moganite content determined by
594 powder X-ray diffraction method. (a) band intensity of the 264 cm^{-1} band; (b) band intensity of

595 the 374 cm^{-1} band; (c) band area of the 576 cm^{-1} band; and (d) band intensity of the 696 cm^{-1}
596 band. The FIR data are from measurements with polyethylene pellets and MIR data from
597 measurements with KBr pellets. The data show that the 374 cm^{-1} band is a characteristic band of
598 quartz which disappears in moganite, whereas the 576 cm^{-1} band is typical band of moganite
599 which does not occur in quartz. Lines are guides to the eye.
600
601 Figure 5. Full width at half maximum (FWHM) of IR bands as a function of moganite content
602 determined by powder X-ray diffraction. (a) the 264 cm^{-1} band; (b) the 374 cm^{-1} band (a
603 characteristic band of quartz); (c) the 576 cm^{-1} band (a characteristic band of moganite); (d) the
604 696 cm^{-1} band; and (e) the 799 cm^{-1} band. Lines are guides to the eye.
605
606 Figure 6. Band wavenumber of the 576 cm^{-1} band as a function of moganite content determined
607 by powder X-ray diffraction.
608
609 Figure 7. (a) Multi-phonon spectrum; and (b) 2nd-deriviative spectrum (between 1300 and 2400
610 cm^{-1}) of moganite thin section (BDL10).
611
612 Figure 8. OH and H_2O absorption in moganite thin sections (BDL10). The inset shows
613 combination bands (at 4388, 4443 and 4515 cm^{-1}) of OH and the 5226 cm^{-1} of H_2O. The first
614 overtone of H_2O and OH are seen near 6828 and 7040 cm^{-1}.

Fig. 1

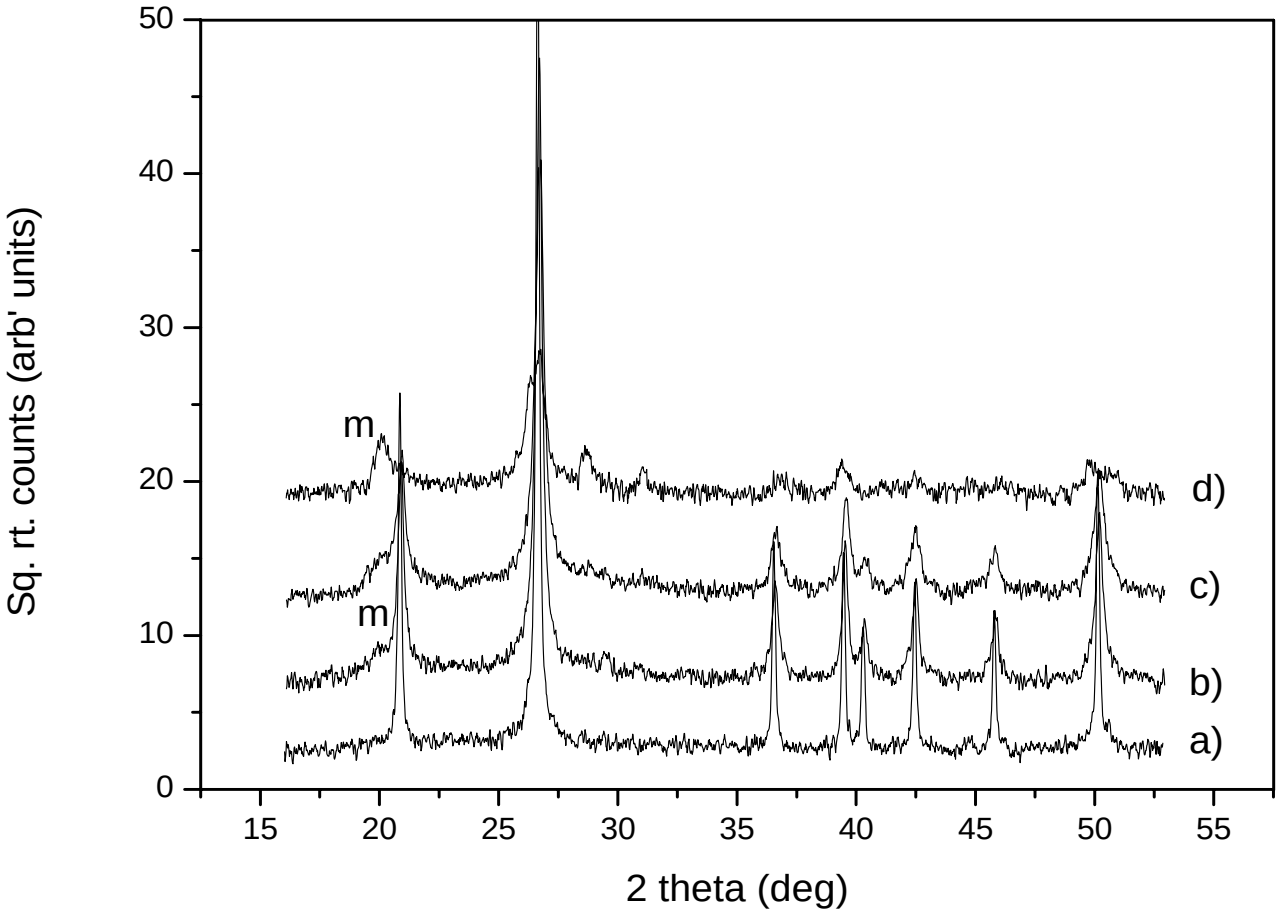
Sq. rt. counts (arb' units)
2 theta (deg)
m
m
d)
c)
b)
a)
0
10
20
30
40
50
15
20
25
30
35
40
45
50
55

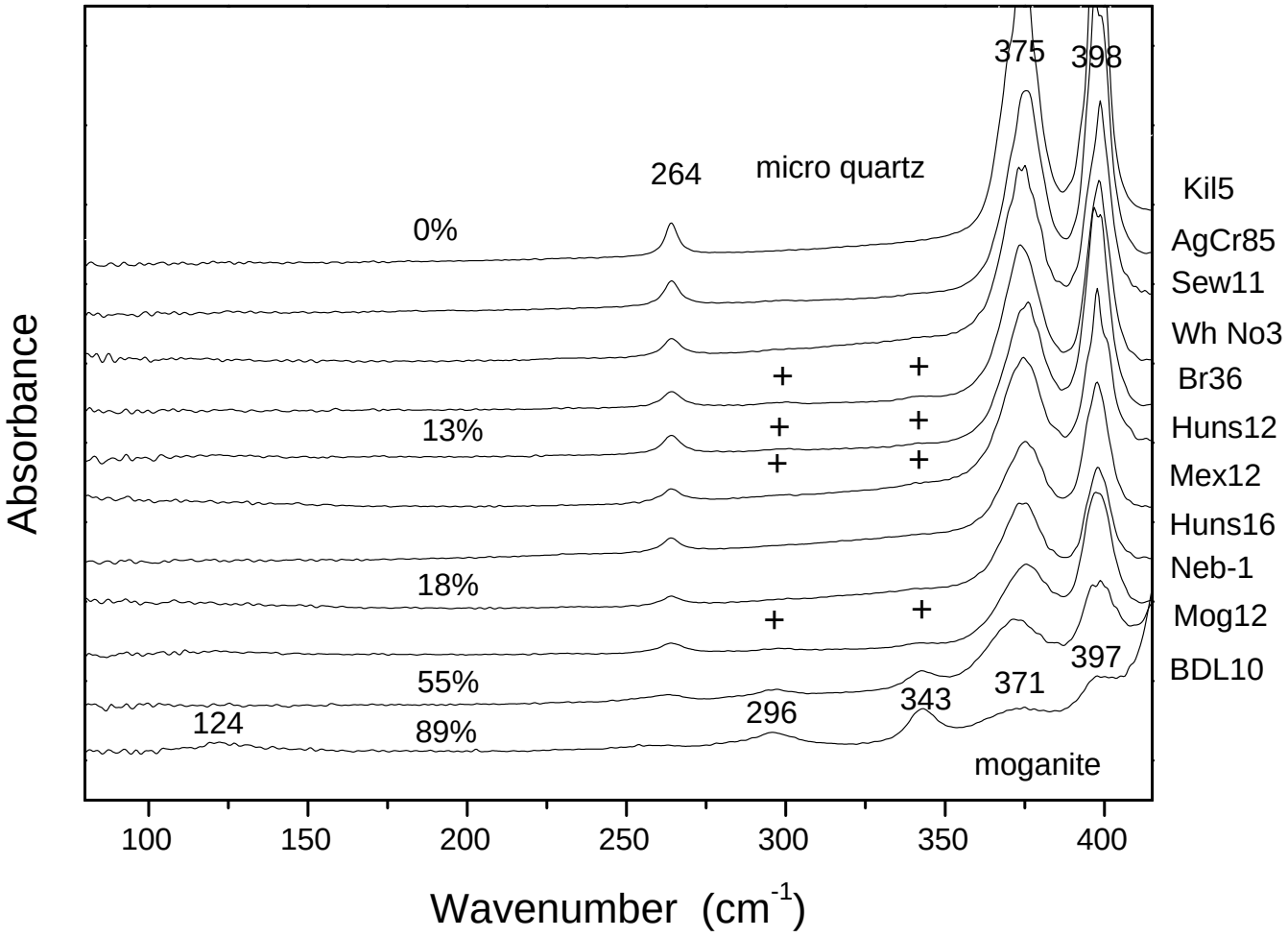
Absorbance
Wavenumber (cm-1)
100
150
200
250
300
350
400
375
398
264
micro quartz
0%
13%
18%
55%
89%
124
296
343
371
397
moganite
Kil5
AgCr85
Sew11
Wh No3
Br36
Huns12
Mex12
Huns16
Neb-1
Mog12
BDL10

Fig. 2b

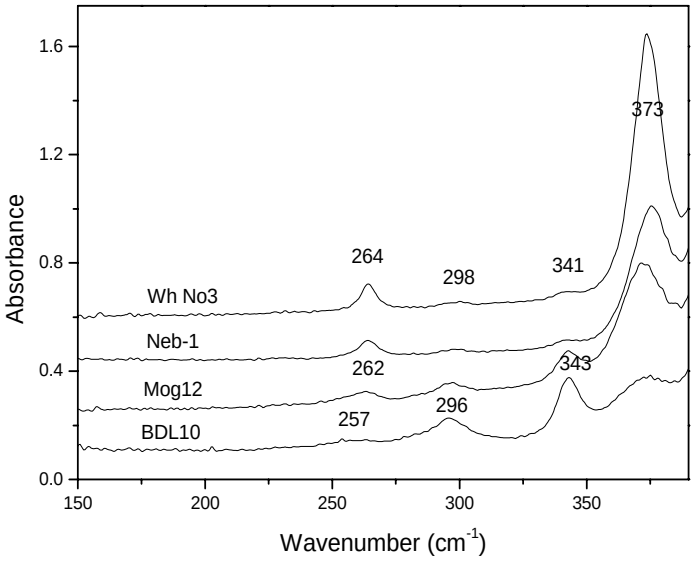
Absorbance
Wavenumber (cm-1)
Wh No3
Neb-1
Mog12
BDL10
264
298
341
373
262
343
257
296

Fig. 2c

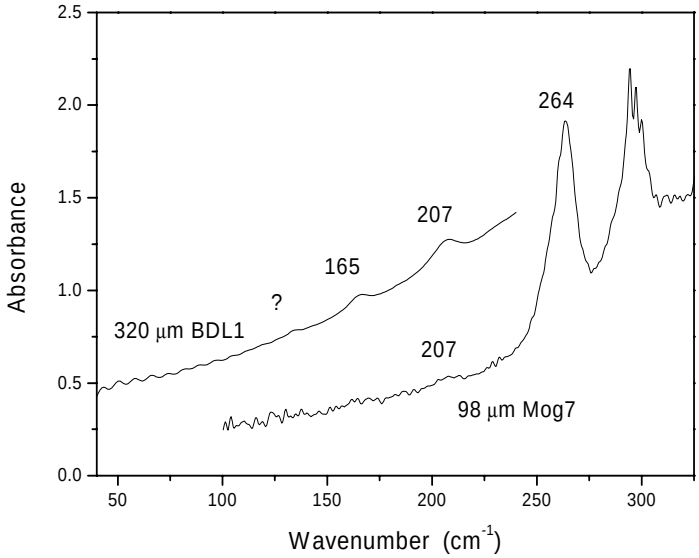
Absorbance
Wavenumber (cm-1)
320 μm BDL1
?
165
207
264
207
98 μm Mog7

Fig. 3a

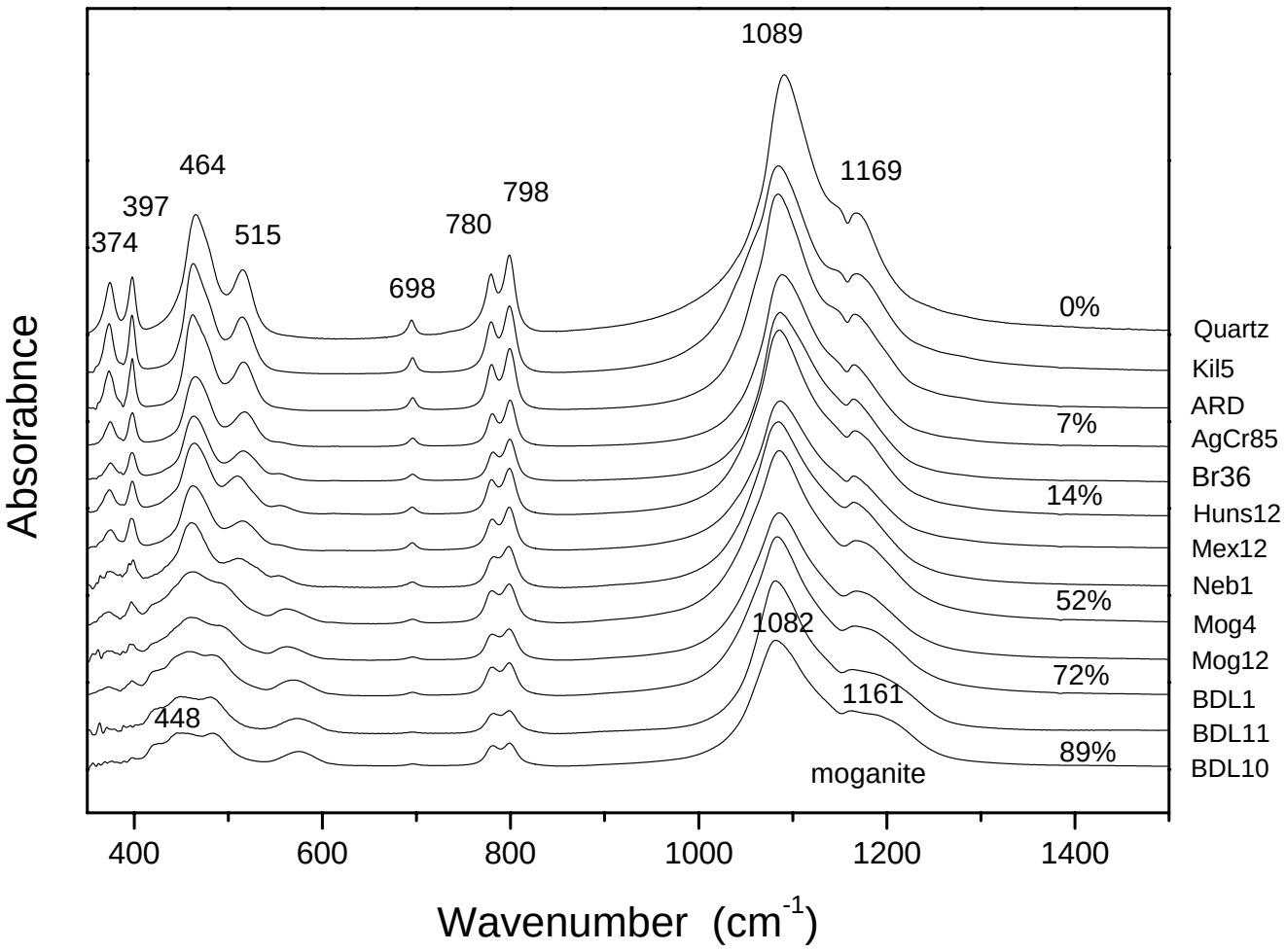
1089
464
397
374
515
780
798
698
1169
0%
Quartz
Kil5
ARD
7%
AgCr85
Br36
14%
Huns12
Mex12
Neb1
52%
Mog4
1082
Mog12
72%
BDL1
1161
448
BDL11
89%
BDL10
moganite
Absorabnce
400
600
800
1000
1200
1400
Wavenumber (cm-1)

This is a preprint, the final version is subject to change, of the American Mineralogist (MSA)
Cite as Authors (Year) Title. American Mineralogist, in press.
(DOI will not work until issue is live.) DOI: http://dx.doi.org/10.2138/am.2014.4589

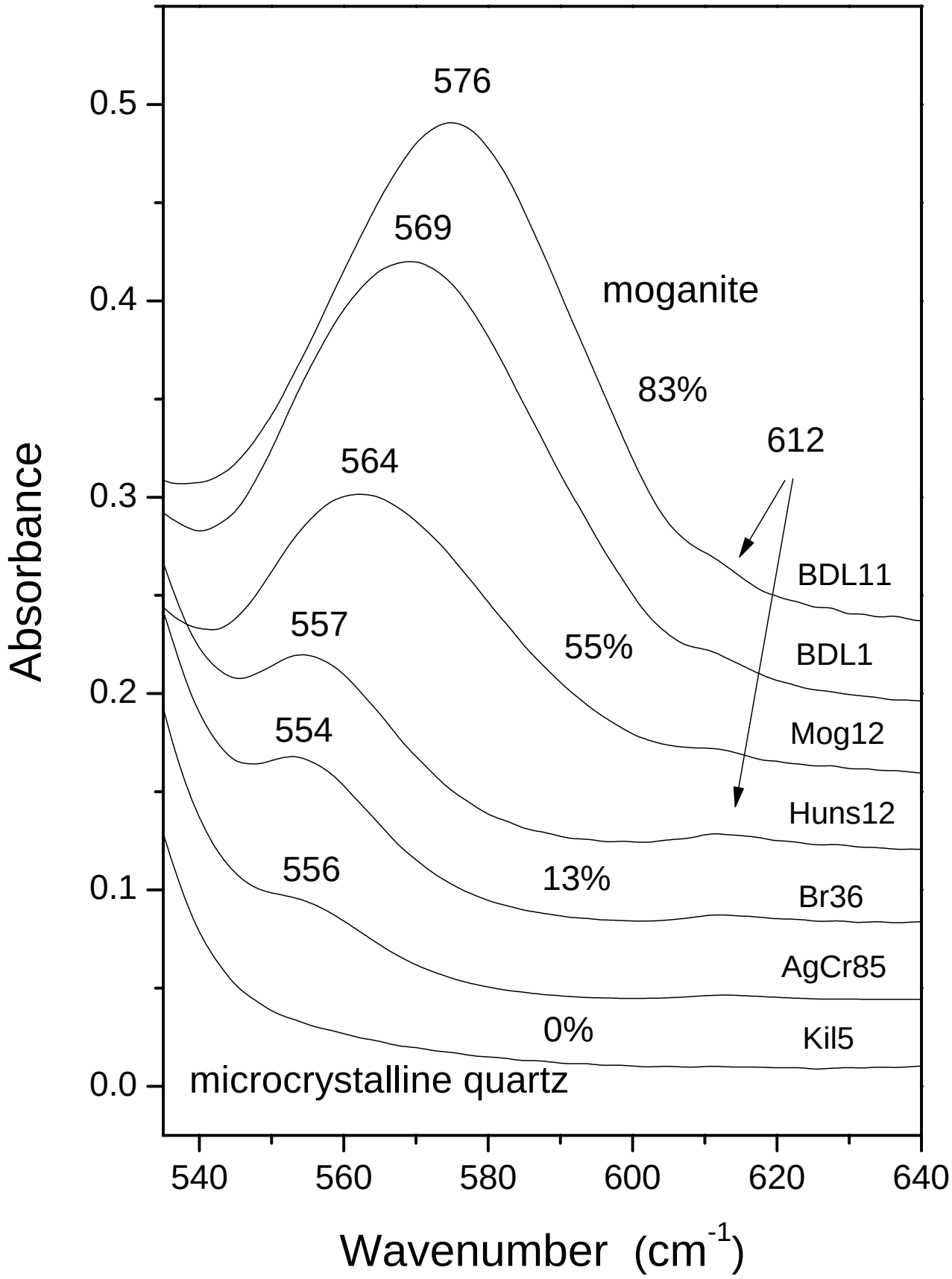

Fig. 4

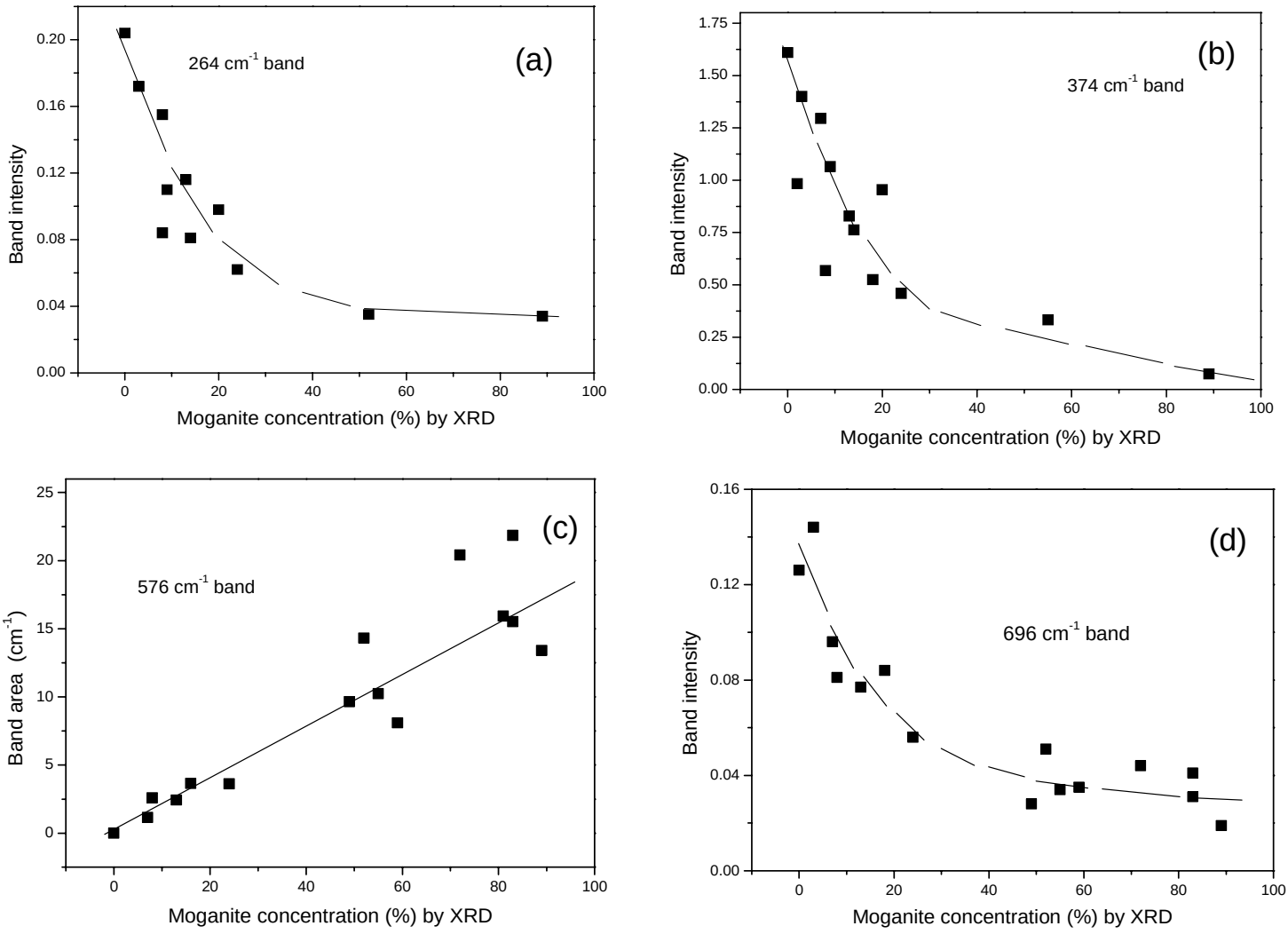
(a)
264 cm-1 band
Band intensity
Moganite concentration (%) by XRD
(b)
374 cm-1 band
Band intensity
Moganite concentration (%) by XRD
(c)
576 cm-1 band
Band area (cm-1)
Moganite concentration (%) by XRD
(d)
696 cm-1 band
Band intensity
Moganite concentration (%) by XRD

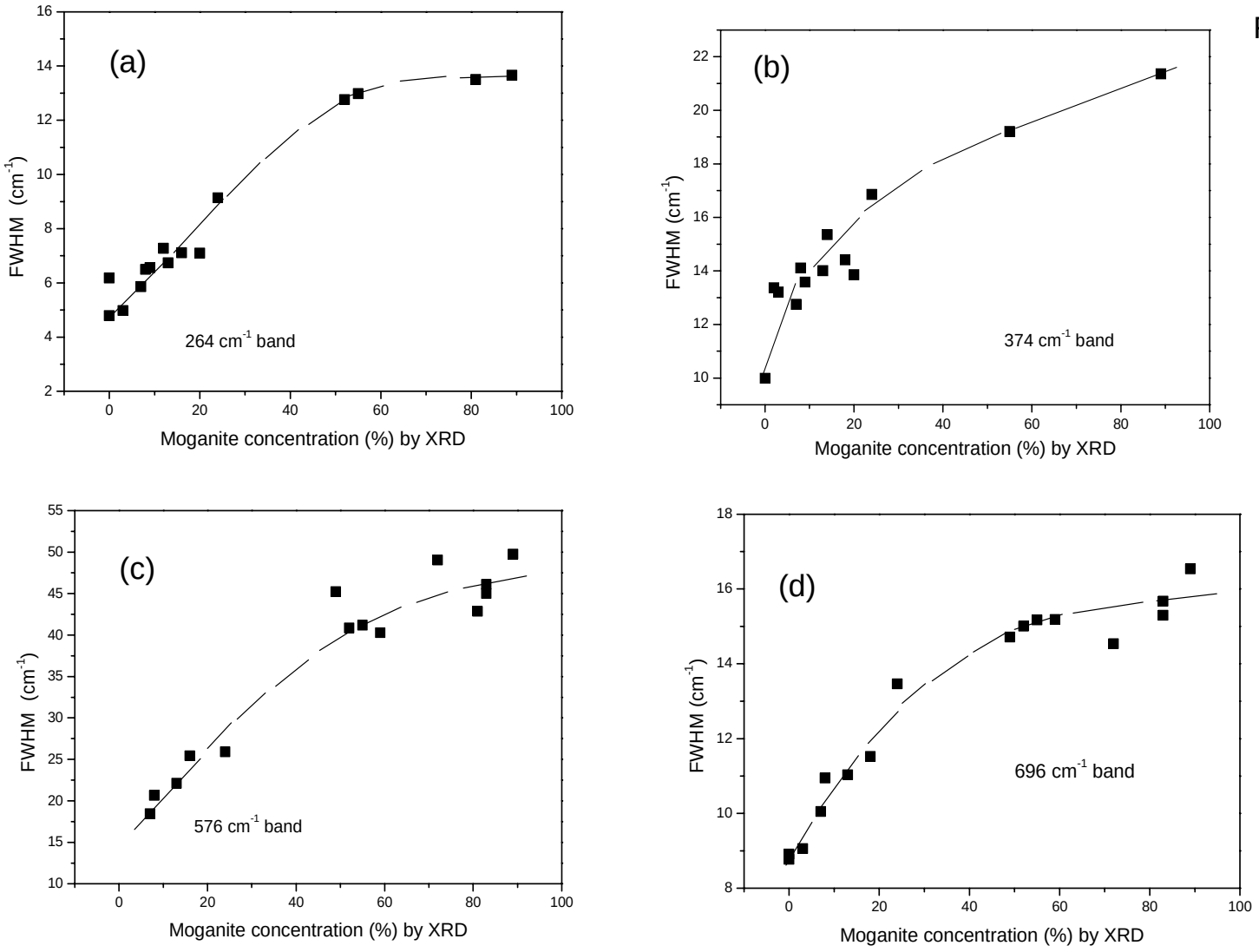
(a)
264 cm-1 band
(b)
374 cm-1 band
(c)
576 cm-1 band
(d)
696 cm-1 band
FWHM (cm-1)
Moganite concentration (%) by XRD

Fig. 5

Fig. 5e

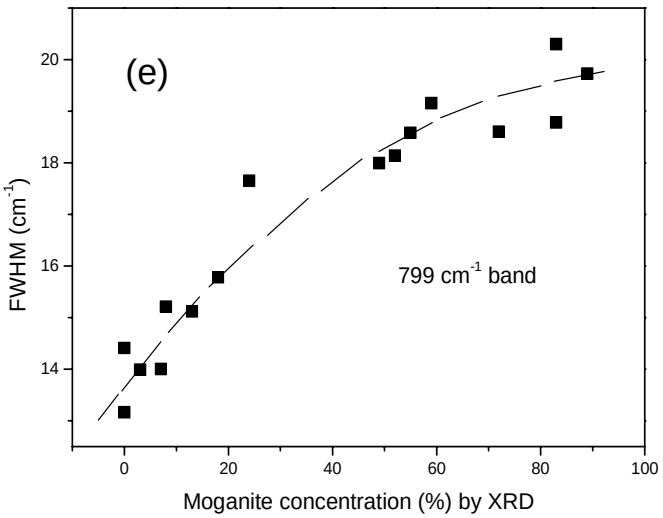
(e)
FWHM (cm-1)
799 cm-1 band
Moganite concentration (%) by XRD

Fig. 6

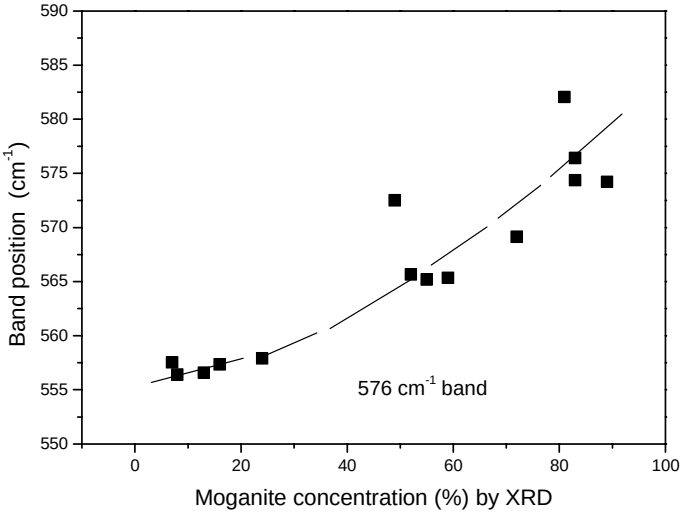
Band position (cm-1)
576 cm-1 band
Moganite concentration (%) by XRD

Fig. 7

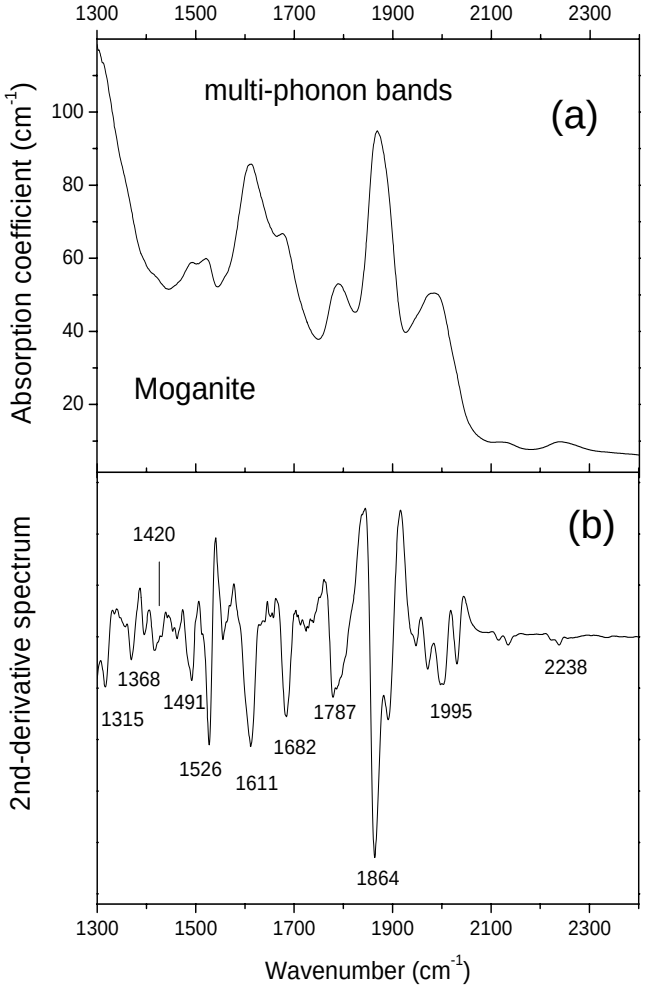
multi-phonon bands
(a)
Moganite
(b)
1420
1368
1315
1491
1526
1611
1682
1787
1864
1995
2238
Absorption coefficient (cm-1)
2nd-derivative spectrum
Wavenumber (cm-1)

Fig. 8

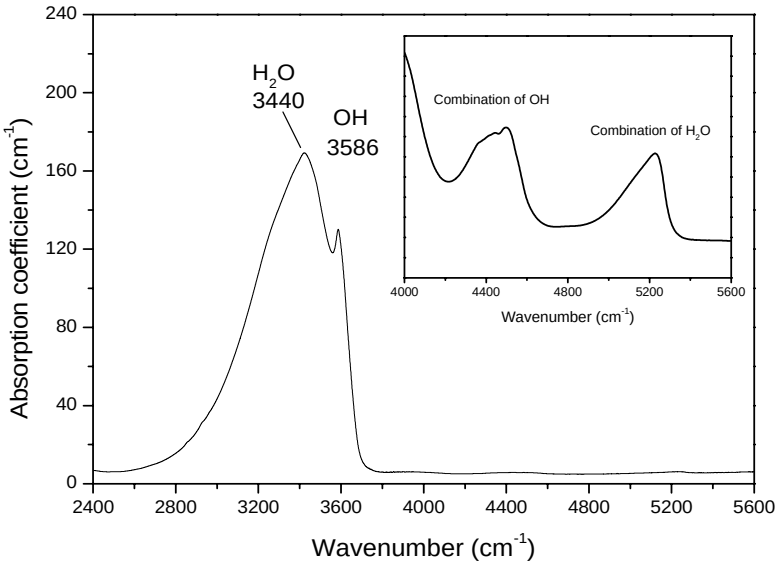
H2O
3440
OH
3586
Combination of OH
Combination of H2O
Absorption coefficient (cm-1)
Wavenumber (cm-1)

Table 1. Sample information. Flint, chert, agate and chalcedony are microcrystalline members of the quartz family which contain moganite.

Samples	Localities	Host	Age of host (Ma) (reference)	Moganite content (%)	Collector
Flint					
Wh No 3	White Nothe, Dorset, England	Chalk	Cretaceous [a]	20	TM
Sew11gr	Sewerby, Yorkshire, England	Chalk	Cretaceous [b]	9	TM
Hun 12	Hunstanton, Norfolk, England	Chalk	Cretaceous [c]	14	TM
Hun 16	Hunstanton, Norfolk, England	Chalk	Cretaceous [c]	18	
Chert					
Der 20	Peak District, Derbyshire, England	Limestone	Carboniferous [d]	< 2	TM
Agate and chalcedony					
Neb 1	Chadron Formation, Nebraska, USA	Siltstone	Eocene [e]	24	RC
Br 36	Soledado Mines, Rio do Sol, Brazil	Basalt	135 [f]	13	purchased
Mex 12	Laguna, Chihuahua, Mexico	Basalt/andesite	38 [e]	8	BC
AgCr 85	Agate Creek, Queensland, Australia	Andesite	275 [e]	7	NC
Ard 7	Ardownie, East Midland Valley, Scotland	Basalt	412 [e]	3	BL
Kil 5	Killara Formation, Killara, Australia	Dolerite	1840 [e]	0	DN
Moganite					
Mog4	Mogan Formation, Mogan, Gran Canaria, Spain	Ignimbrite	13 [g]	52	PH, JP
Mog7	Mogan Formation, Mogan, Gran Canaria, Spain	Ignimbrite	13 [g]	81	PH, JP
Mog11	Mogan Formation, Mogan, Gran Canaria, Spain	Ignimbrite	13 [g]	49	PH, JP
Mog12	Mogan Formation, Mogan, Gran Canaria, Spain	Ignimbrite	13 [g]	55	PH, JP
BDL1	Barranco de los Frailes, Gran Canaria, Spain	Ignimbrite	13 [g]	72	PH, JP
BDL2	Barranco de los Frailes, Gran Canaria, Spain	Ignimbrite	13 [g]	59	PH, JP
BDL11	Barranco de los Frailes, Gran Canaria, Spain	Ignimbrite	13 [g]	83	PH, JP
BDL12	Barranco de los Frailes, Gran Canaria, Spain	Ignimbrite	13 [g]	83	PH, JP
BDL10 white powder	Barranco de los Frailes, Gran Canaria, Spain	Ignimbrite	13 [g]	89	PH, JP
BDL10	Barranco de los Frailes, Gran Canaria, Spain	Ignimbrite	13 [g]	89	PH, JP
Standard quartz					
Quartz	Synthetic			0	purchased

a) House (1989); b) Kent (1980); c) Rawson (1992); d) Stevenson and Gaunt (1971); e) references are given in Moxon and Carpenter (2009); f) Pinto et al. (2011); g) Kobberger and Schminke (1999). TM = Terry Moxon; RC = Roger Clark, BC = Brad Cross, NC = Nick Crawford, BL = Brian Leith, DN = Dave Nelson, PH = Peter Heaney, and JP = Jeffrey Post.

Table 2. Infrared absorption modes of moganite, microcrystalline quartz, macrocrystalline quartz, cristobalite and tridymite.

Moganite (this work)	Moganite [a]	Moganite [b]	Micro quartz * (this work)	Quartz * (this work)	Cristobalite [c]	Tridymite [d]
127 (very weak)			128	128(E) [e]		
					145	
165						
207						
257 (or 264)			264	264(E)	275	
296	295					298
343	341					
			373	374(A_2)	380	
			398	397(E)		394
421	420	418				
448	447	447			445	
			463	464(E)		
483	480	480			485	488
						495
			515	514(A_2)		
576	572	570 (weak)				
612 (weak)		600 (strong)			620	617
696		700	696	698(E)		
780		800	779	780(A_2)	785	
798	800	808	798	798(E)		800
1082	1100	1105	1085	1089(A_2)	1086	1070
			1148	1148(LO?)		
1167			1168	1169(E)	1162	
1191(shoulder)		1191			1195	1220

a - Miehe & Graetsch (1992), b - Parthasarathy et al. (2001), c - Zhang and Scott (2007), d - Plendl et al. (1967), and e - band species from Scott and Porto (1967). Please note that the IR bands of tridymite are sensitive to experimental conditions as shown by Cellai et al. (1995).
* Micro quartz = microcrystalline quartz, and Quartz = macrocrystalline quartz. The analysis error for band position is less than 1 cm^{-1} in the present work.

Table 3. Tentative assignments of main multi-phonon absorptions of moganite.

Observed	Calculated	Tentative assignments
1315	257+1082 =1339	Si-O-Si bend + Si-O stretch
1420	343+1082 =1425	Si-O-Si bend + Si-O stretch
1496	696 +798 =1494	Si-O stretch + Si-O stretch
1526	448+1082 =1530	Si-O-Si bend + Si-O stretch
1611	448+1167 =1615	Si-O-Si bend + Si-O stretch
1682	483+1191=1674	Si-O-Si bend + Si-O stretch
1787	696+1082=1778	Si-O stretch + Si-O stretch
1864	696+1167 =1863	Si-O stretch + Si-O stretch
1995	798+1191=1989	Si-O stretch + Si-O stretch
2238	1082+1167=2249	Si-O stretch + Si-O stretch